Normal-state properties of high-temperature superconductors

Hongguang Chi and A. D. S. Nagi
Guelph-Waterloo Program for Graduate Work in Physics, Department of Physics, University of Waterloo, Waterloo, Ontario, Canada N2L 3G1
(Received 30 July 1991; revised manuscript received 27 March 1992)

The doping and the temperature dependence of various normal-state properties of high-temperature superconductors are studied by applying the t-t'-J model. The slave-boson method is used to treat the strong correlations. The fermion quasiparticles carry both charge and spin and the volume of the Fermi surface satisfies the Luttinger theorem. The quasiparticle energy spectrum used in the calculation is obtained from a mean-field treatment of the t-t'-J model. The study is confined to the metallic phase where contributions from the t and t' terms are most dominant. The calculations provide a quantitative understanding for the doping dependence of Drude plasma frequency, Hall resistivity R_H, band Pauli magnetic susceptibility χ_{SB}, thermopower, and the room-temperature dc conductivity. The temperature dependence of R_H and χ_{SB} for small doping are not understood. The calculated density of states, Fermi energy, effective mass, and the Sommerfeld parameter have reasonable values. We have taken $J=0$ and $t=0.45$ eV and have considered a wide range of t' values.

I. INTRODUCTION

The normal-state properties of high-temperature superconductors (HTSC) are anomalous and may provide the most important clue to their physics.[1,2] Anderson[3] has pointed out that the single-band Hubbard model should be a good starting point to understand the physics of HTSC. In the large intrasite Coulomb repulsion limit, the Hubbard Hamiltonian reduces to a single-band effective Hamiltonian, known as the t-J Hamiltonian. Anderson[4] has reemphasized that the single-band effective Hamiltonian is adequate even in the light of multiband proposals.[5-7] Zhang and Rice[8] have derived the single-band effective Hamiltonian starting from a two-band model. Kotliar, Lee, and Read[9] arrived at the same result. More recently, semiempirical analysis[10] and constrained local-density-functional (LDA) calculations[11] also support the above conclusion. The t-t'-J model is an extension of the t-J model by including the next-nearest-neighbor hopping term.[12]

Starting with the t-J (or t-t'-J) model, a number of problems related with the physics of the oxide superconductors have been studied. As the undoped oxides are quantum antiferromagnets (e.g., $La_{2-x}Sr_xCuO_4$ with $x=0$), one of the important problems is to consider a hole (carrying charge and spin) moving in a quantum antiferromagnet.[13-19] In fact, the problem of a hole moving in an Ising antiferromagnetic background was considered several years ago by Brinkman and Rice[13] who employed a self-retracing-path approximation. The basic idea of this approximation is that the hopping of a hole in a Neel state will create a "string" of overturned spins along its path and in order to return the spin configuration to its original state, one should consider paths in which the hole retraces its path back to the origin. A significant result of such studies is that in the self-retracing path approximation the hole is always localized.[13,14] To delocalize the hole, one needs either to turn on the quantum fluctuations[16,17] or to include the "loop paths."[15,18] Recently, the quasiparticle dispersion relation obtained from the hole-motion problem has been used by Trugman[20] for calculating some normal state properties of HTSC. Specifically, he assumed that the quasiparticles fill the rigid band described by the single-hole dispersion relation and that they form a weakly interacting Fermi gas. A good quantitative agreement with experiment was obtained in Ref. 20. Trugman has chosen that $t=1.6$ eV and $t'=J=0.133$ eV. One of important results of the Trugman theory is that the Fermi surface consists of eccentric ellipses and the volume enclosed by the Fermi surface is proportional to x (hole concentration). It may be mentioned that angle-resolved photoemission, angle-resolved inverse photoemission, and positron-annihilation two-dimensional angular correlation of annihilation radiation measurements[21] seem to indicate a Fermi surface that includes an area proportional to $1-x$ (satisfying the Luttinger Theorem). The issue of the nature of the Fermi surface is not resolved at present and more accurate measurements are needed. More recent theoretical studies of the Fermi surface are given in Ref. 22.

Recognizing the importance of satisfying the Luttinger theorem, Nagoasa and Lee[23] have calculated the normal state properties of HTSC by developing a gauge-field-theory approach. They studied a resonating-valence-bond (RVB) state[3,24] in which fermions (spinons) and spinless bosons (holons) are coupled by a gauge field and the spinon Fermi surface obeys the Luttinger theorem. They assumed that the doping level is sufficiently large to stabilize the uniform RVB state. Their approach is partially based on Refs. 25 and 26 where gauge fields are considered in detail. The authors of Ref. 23 were able to understand the linear T resistivity and they also found that the Hall number is proportional to the hole density and is temperature dependent.

Anderson and Ren[27] have recently proposed that the normal state of HTSC is a new metallic state known as

"Luttinger liquid"—the basic idea is that the systems described by the 2D Hubbard model are "Luttinger liquids." In the "Luttinger liquid" state, which was developed from the study of a 1D interacting electron system, the charge and spin acquire distinct spectra and the Fermi surface correlations have unusual exponents. Thus the charge and spin are deconfined. While interesting results have been obtained for 1D systems,[28,29] generalization to 2D systems is very difficult.

The two-band Hubbard model or the CuO_2 model has also been used to study the normal state properties of HTSC. This model considers holes in the $3d$ orbital of copper and $2p$ orbitals of oxygen and is characterized by the set of parameters $(B,t_p,t_d,U_{dd},U_{pp},J,V)$ with $B=(\varepsilon_p,\varepsilon_d-\varepsilon_p,t_{pd})$ as the basic set. Here $\varepsilon_d-\varepsilon_p$ is the d-p splitting energy (or the charge transfer energy), V is the intersite Coulomb repulsion and the other parameters have their conventional meanings. Newns and coworkers have studied the case of $(B,t_p,0,\infty,0,0,0)$ (Ref. 30) and $(B,t_p,t_d,\infty,0,0,0)$ (Ref. 31) for a small value of $\varepsilon_d-\varepsilon_p$. Kim, Levin, and Auerbach[32] (KLA) considered $(B,t_p,0,\infty,0,0,0)$ with several different values of $\varepsilon_d-\varepsilon_p$. Castellani and Kotliar[33] considered the case $(B,0,0,\infty,0,J,0)$ and studied the phase transition from the Fermi-liquid to the non-Fermi-liquid state. Balserio *et al.*[34] investigated $(B,0,0,U_{dd},U_{pp},0,V)$. Grilli, Kotliar, and Millis[35] (GKM) studied $(B,t_p,0,\infty,0,J,V)$ and presented a systematic analysis. All the above studies use mean-field theory approach. We will compare our results with those from above studies whenever possible.

Varma *et al.*[36] have developed a marginal-Fermi-liquid theory for the normal state of HTSC. Assuming that there exist charge- and spin-density excitations with the imaginary part of the polarizability at low frequencies ω proportional to ω/T and constant otherwise, they have understood the temperature dependence of several properties. Ruvalds and Virosztek[37] have studied the optical properties of these oxides by considering Fermi-surface nesting. Schneider and Sörensen[38] have investigated some normal state properties using a tight-binding band.

In the present paper, we have calculated the doping and the temperature dependence of several normal state properties of HTSC by using quasiparticles with energy spectrum derived from a mean-field treatment of the t-t'-J model. The quasiparticles carry both charge and spin and the volume of the Fermi surface satisfies the Luttinger theorem. We have employed the slave-boson method to treat the strong correlations. Our study deals with the metallic phase for which the transfer integral terms are most dominant and consequently the superexchange term has been ignored.

The paper is organized as follows: Section II gives a general formalism. Starting with t-t'-J model and using the slave-boson method, the energy spectrum of the quasiparticles is obtained within the mean-field approximation. An electron-hole interaction term, which is believed to be responsible for the anomalous relaxation time of the carriers, is also obtained. Further, the formulas for calculating various transport properties are given in this section. In Sec. III, we present detailed numerical results of the transport properties. First, the Fermi-surface related properties and the Drude plasma frequency at zero temperature are given. Next, at room temperature, the doping dependence of the Hall resistivity, band Pauli magnetic susceptibility, thermopower, and dc conductivity are shown. Finally, the temperature dependence of the above transport properties are presented. Section IV gives a summary and discussions.

II. FORMALISM

The t-t'-J model is an extension of the t-J model by including the next-nearest-neighbor hopping term.[12] The t-J model has been derived from the single-band Hubbard model in the large-intrasite-Coulomb-repulsion-(U) limit in Refs. 39–41. The derivation of the t-J model from a two-band model was carried out by Zhang and Rice.[8] The t-t'-J model is described by the Hamiltonian

$$H=-t\sum_{\langle i,j\rangle,\sigma}h_{i\sigma}^{\dagger}h_{j\sigma}+t'\sum_{\langle i,j\rangle,\sigma}h_{i\sigma}^{\dagger}h_{j\sigma}+J\sum_{\langle i,j\rangle}\left[\boldsymbol{\sigma}_i\cdot\boldsymbol{\sigma}_j-n_in_j\right], \tag{1}$$

where t,t', respectively, are the transfer integrals for the nearest neighbor (NN) and the next nearest neighbors (NNN) and J is the superexchange interaction. The first (second) summation is over NN (NNN). The operators $h_{i\sigma}$ hop single electrons from site to site but are not true fermion operators since they are subject to the single occupancy constraint $h_{i\sigma}^{\dagger}h_{i\sigma}\le 1$. Further $\boldsymbol{\sigma}_i$ and n_i, respectively, are the spin density and the number density at site i. For the metallic phase considered in this paper, the contributions from transfer integral terms are most dominant and the J term can be neglected.

A convenient way to deal with the single occupancy constraint is to use the slave-boson technique.[42,43] In this technique, one writes

$$h_{i\sigma}=C_{i\sigma}b_i^{\dagger}, \tag{2}$$

where $C_{i\sigma}$ is a fermion operator (which carries the spin quantum number σ and the charge) and b_i is the boson operator (which keeps track of the empty sites). Usually $C_{i\sigma}$ and b_i, respectively, are referred to as the electron and the hole operators. Using Eq. (2) in Eq. (1) and taking $J=0$, one gets[44]

$$H=-t\sum_{\langle i,j\rangle,\sigma}b_i^{\dagger}b_jC_{j\sigma}^{\dagger}C_{i\sigma}+t'\sum_{\langle i,j\rangle,\sigma}b_i^{\dagger}b_jC_{j\sigma}^{\dagger}C_{i\sigma}. \tag{3}$$

Further, in the slave-boson method, the single-occupancy-constraint inequality for site i is converted to the holonomic constraint

$$\sum_{\sigma}C_{i\sigma}^{\dagger}C_{i\sigma}+b_i^{\dagger}b_i=1. \tag{4}$$

This constraint is treated in the mean-field approximation; i.e., we replace Eq. (4) by

$$\langle b_i^{\dagger}b_i\rangle=x, \qquad \sum_{\sigma}\langle C_{i\sigma}^{\dagger}C_{i\sigma}\rangle=1-x, \tag{5}$$

where x is the occupation number for holes. Our calculations based on Eq. (3) are mainly for the $La_{2-x}Sr_xCuO_4$ system but apply to other "p-type" HTSC compounds if the relevant physics occurs in the CuO_2 planes.

In the momentum space, Eq. (3) becomes

$$H=-\frac{1}{N}\sum_{\mathbf{p},\mathbf{q},\mathbf{k},\sigma} f(\mathbf{p}-\mathbf{k})b_{\mathbf{k}}^{\dagger}b_{\mathbf{k}+\mathbf{q}}C_{\mathbf{p}+\mathbf{q},\sigma}^{\dagger}C_{\mathbf{p},\sigma} , \tag{6}$$

$$f(\mathbf{p})=2t(\cos p_x a+\cos p_y a -2t'/t\cos p_x a\cos p_y a) , \tag{7}$$

with a as the lattice spacing. Similarly Eqs. (5) become

$$\frac{1}{N}\sum_{\mathbf{k}} n_{\mathbf{k}}^{h}=x , \tag{8}$$

$$\frac{1}{N}\sum_{\mathbf{p},\sigma} n_{\mathbf{p},\sigma}^{e}=1-x , \tag{9}$$

where $n_{\mathbf{k}}^{h}=\langle b_{\mathbf{k}}^{\dagger}b_{\mathbf{k}}\rangle$ and $n_{\mathbf{p},\sigma}^{e}=\langle C_{\mathbf{p},\sigma}^{\dagger}C_{\mathbf{p},\sigma}\rangle$. Carrying out a self-consistent Hartree-Fock factorization for the nonscattering ($q=0$) terms, Eq. (6) gives

$$H=H_e+H_h+H_{\rm int} , \tag{10}$$

with

$$H_e=\sum_{\mathbf{p},\sigma}(\varepsilon_{\mathbf{p}}-\mu^e)C_{\mathbf{p},\sigma}^{\dagger}C_{\mathbf{p},\sigma} , \tag{11}$$

$$H_h=\sum_{k}(\varepsilon_{\mathbf{k}}^{h}-\mu^h)b_{\mathbf{k}}^{\dagger}b_{\mathbf{k}} , \tag{12}$$

$$H_{\rm int}=-\frac{1}{N}\sum_{\mathbf{p},\mathbf{k},\mathbf{q}\neq 0,\sigma} f(\mathbf{p}-\mathbf{k})b_{\mathbf{k}}^{\dagger}b_{\mathbf{k}+\mathbf{q}}C_{\mathbf{p}+\mathbf{q},\sigma}^{\dagger}C_{p,\sigma} . \tag{13}$$

Here, the $H_{\rm int}$ term represents the electron-hole interaction. It can lead to superconducting pairing[45] and is also believed to be responsible for the anomalous relaxation time τ of the carriers. Also $\varepsilon_{\mathbf{p}}$ and $\varepsilon_{\mathbf{k}}^{h}$, respectively, are the energy spectrum for the electrons and holes, and are given by

$$\varepsilon_{\mathbf{p}}=-\frac{1}{N}\sum_{\mathbf{k}} f(\mathbf{p}-\mathbf{k})\langle b_{\mathbf{k}}^{\dagger}b_{\mathbf{k}}\rangle , \tag{14}$$

$$\varepsilon_{\mathbf{k}}^{h}=-\frac{1}{N}\sum_{\mathbf{p},\sigma} f(\mathbf{p}-\mathbf{k})\langle C_{\mathbf{p},\sigma}^{\dagger}C_{\mathbf{p},\sigma}\rangle . \tag{15}$$

Further, μ^e and μ^h, respectively, are the chemical potentials for the electrons and the holes and are used to enforce that the occupation numbers of electrons and holes satisfy Eqs. (8) and (9).

As holes are light bosons and x is a small fraction, one expects that small values of $\mathbf{k}$ dominate so that Eq. (14) can be approximated as

$$\varepsilon_p\simeq -2tx(\cos p_x a+\cos p_y a -2t'/t\cos p_x a\cos p_y a) , \tag{16}$$

where Eqs. (7) and (8) have also been used. This energy spectrum has the form of a tight binding band renormalized by the strong correlations. It can also be obtained from Eq. (3) by replacing b_i with its mean-field value $\langle b_i\rangle=x^{1/2}$. It may be noted that this replacement of the bosons by a c-number amounts to the assumption of Bose condensation of the b's. The energy spectrum implies that the bandwidth increases and the effective mass decreases with the increase of hole concentration. It especially gives the Brinkman-Rice[46] (Coulomb) localization as x approaches zero.

Normal-state transport properties can be obtained by using standard formulas.[47,48] Using Eq. (16), various transport coefficients in the constant-relaxation-time approximation are given by

$$\sigma_{xx}=\frac{2\tau}{l_c}\left[\frac{\rm ext}{\pi\hbar}\right]^2\int\int_{\rm LB} d\tilde{p}_x d\tilde{p}_y \sin^2\tilde{p}_x(1-2t'/t\cos\tilde{p}_y)^2(-\partial f/\partial\varepsilon_{\tilde{p}}) , \tag{17}$$

$$\sigma_{xyz}=-\frac{({\rm ext})^3}{l_c}\left[\frac{2\tau a}{\pi\hbar^2}\right]^2\int\int_{\rm LB} d\tilde{p}_x d\tilde{p}_y f_{xyz}(-\partial f/\partial\varepsilon\tilde{p}) , \tag{18}$$

$$S=S_{xx}=-\frac{k_B}{e}\int_{\rm LB} d\varepsilon\left[\frac{\varepsilon-\mu^e}{k_B T}\right]\sigma_{xx}(\varepsilon)(-\partial f/\partial\varepsilon)/\int_{\rm LB} d\varepsilon\,\sigma_{xx}(\varepsilon)(-\partial f/\partial\varepsilon) . \tag{19}$$

In the above equations

$$f_{xyz}=\sin^2\tilde{p}_x(1-2t'/t\cos\tilde{p}_x)(1-2t'/t\cos\tilde{p}_y)(\cos\tilde{p}_y-2t'/t) , \tag{20}$$

$$\sigma_{xx}(\varepsilon)=\frac{2\tau}{l_c}\left[\frac{ext}{\pi\hbar}\right]^2\int\int_{\rm LB} d\tilde{p}_x d\tilde{p}_y(1-2t'/t\cos\tilde{p}_y)^2\sin^2\tilde{p}_x\delta(\varepsilon_{\tilde{p}}-\varepsilon) . \tag{21}$$

Here, σ_{xx} is the dc conductivity in the CuO_2 plane, σ_{xyz} is related to the Hall resistivity R_H given by $R_H=R_{xyz}=\sigma_{xyz}/\sigma_{xx}^2$, and S is the thermopower. Further, τ is the quasiparticle relaxation time, l_c is the distance between the two neighboring CuO_2 planes, $\tilde{p}_x=p_x a$,

$$f=f(\varepsilon_{\tilde{p}})=\{\exp[(\varepsilon_{\tilde{p}}-\mu^e)/k_B T]+1\}^{-1}$$

is the Fermi function, and the notation LB is the lower Mott-Hubbard band whose upper edge ε_u is determined by

$$\frac{2}{N}\sum_{\mathbf{p}}\Theta(\varepsilon_{\mathbf{p}}-\varepsilon_u)=1 . \tag{22}$$

Both the Hall resistivity and the thermopower are independent of τ.

The band Pauli magnetic susceptibility χ_{SB} is given by

$$\chi_{SB}=\frac{\mu_B^2}{2\pi^2 l_c a^2}\int\int_{\mathrm{LB}} d\tilde{p}_x d\tilde{p}_y(-\partial f/\partial\varepsilon_{\tilde{p}}) , \tag{23}$$

where μ_B is Bohr magneton. The total magnetic susceptibility is the sum of χ_{SB}, the core χ_{core}, the van Vleck χ_{vv}, and χ_J due to the exchange interaction which is not treated here.

The density of states of single quasiparticles of energy ε per Cu site is given by

$$N(\varepsilon)=\frac{2}{N}\sum_{\mathbf{p}}\delta(\varepsilon_{\mathbf{p}}-\varepsilon)$$

$$=\frac{1}{4\pi^2 xt}\int_{\varepsilon_{\mathbf{p}}=\varepsilon}\frac{d\tilde{p}_x}{\left|\sin\tilde{p}_y(1-2t'/t\cos\tilde{p}_x)\right|} . \tag{24}$$

From $N(\mu^e)$, the Sommerfeld parameter γ is calculated by using

$$\gamma=\pi^2 k_B^2 N(\mu^e)/3 . \tag{25}$$

Defining the effective mass m_γ from the theoretical specific heat by assuming a two-dimensional parabolic band, its ratio to the free electron mass is given by

$$\frac{m_\gamma}{m_0}=\frac{\gamma}{\gamma_0}=\frac{\gamma}{2}(1-x)^{3/2} , \tag{26}$$

where γ is measured in units of mJ/mole K^2.

Now we give some details for evaluating ε_u and μ^e. We rewrite Eqs. (9) and (22), respectively, as

$$\frac{1}{\pi^2 xt}\int_{\varepsilon_L}^{\varepsilon_u}d\varepsilon\int_{p_x^{\min}(\varepsilon)}^{p_x^{\max}(\varepsilon)}d\tilde{p}_x\frac{f(\varepsilon)}{\left|\sin\tilde{p}_y(1-2t'/t\cos\tilde{p}_x)\right|}$$

$$=1-x,\quad \tilde{p}_x\geq o,\tilde{p}_y\geq 0 , \tag{27}$$

$$\frac{1}{\pi^2 xt}\int_{\varepsilon_L}^{\varepsilon_u}d\varepsilon\int_{p_x^{\min}(\varepsilon)}^{p_x^{\max}(\varepsilon)}d\tilde{p}_x\frac{1}{\left|\sin\tilde{p}_y(1-2t'/t\cos\tilde{p}_x)\right|}$$

$$=1,\quad \tilde{p}_x\geq 0,\tilde{p}_y\geq 0 , \tag{28}$$

where $p_x^{\min}(\varepsilon)$ and $p_x^{\max}(\varepsilon)$, respectively, are the minimum and the maximum values of p_x on the curve $\varepsilon_{\mathbf{p}}=\varepsilon(\tilde{p}_x\geq 0,\tilde{p}_y\geq 0)$ and are given by

$$p_x^{\min}(\varepsilon)=\begin{cases}\cos^{-1}(W), & |W|<1 ,\\ 0, & |W|>1 ,\end{cases} \tag{29}$$

$$p_x^{\max}(\varepsilon)=\begin{cases}\cos^{-1}(Y), & |Y|<1 ,\\ \pi, & |Y|>1 ,\end{cases} \tag{30}$$

with

$$W=\frac{(1-\varepsilon/2xt)}{(1+2t'/t)} , \tag{31}$$

$$Y=\frac{-(1+\varepsilon/2xt)}{(1-2t'/t)} . \tag{32}$$

The quantity ε_L is the lower edge of the LB. From Eq. (16), one finds that

$$\varepsilon_L=\begin{cases}-4tx(1-t'/t), & t'/t\leq 0.5 ,\\ -4t'x, & t'/t\geq 0.5 .\end{cases} \tag{33}$$

The quantity ε_u is determined from Eq. (28). Then μ^e is obtained by solving Eq. (27). The integrations in Eqs. (17)–(19) and (23) can be carried out similarly and the numerical work is very accurate.

III. NUMERICAL RESULTS

We will present our numerical results in three parts. In Sec. III A, we give the doping dependence of some properties at zero temperature. In Sec. III B, the transport properties at room temperature are presented. In Sec. III C, the doping dependence of the transport properties at several different temperatures are shown.

A. Some properties at zero temperature

Here we study the following properties at zero temperature: Fermi surface, density of states and effective mass at the Fermi energy, Fermi energy, and the Drude plasma frequency.

The Fermi surface is calculated from Eq. (16) and the zero-temperature version of Eq. (27) [i.e., replacing $f(\varepsilon)$ by $\Theta(\mu^e-\varepsilon)$]. Our results at different concentration of holes with $x=0.1$, 0.2, 0.3, 0.4, 0.5, and 0.6 are shown in Fig. 1. We have taken $t'/t=0.30$. It should be noted that the Fermi surface satisfies the Luttinger theorem, i.e., the total volume included by the Fermi surface is proportional to $1-x$ with and without the Coulomb repulsion. However theories with carriers proportional to x (e.g., Ref. 20) do not satisfy the Luttinger theorem. One also notes that the Fermi surfaces are extremely anisotropic. The effective mass of an electron is larger for $\mathbf{p}$ along the axes than along the diagonal. The density of states for an electron in the LB is calculated from Eq. (24)

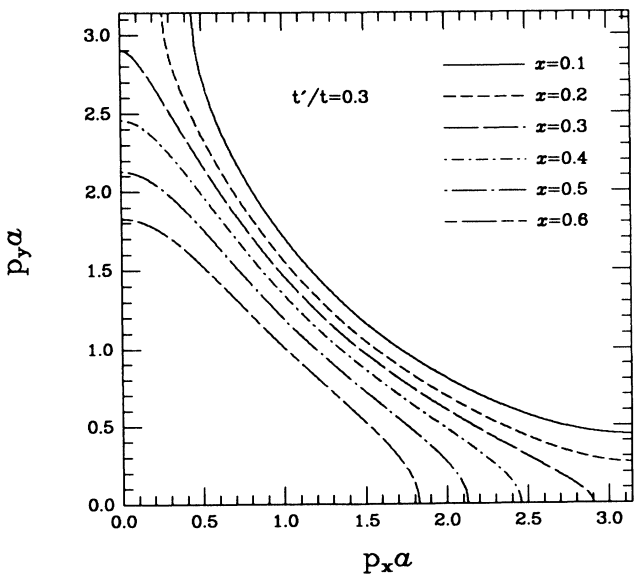

FIG. 1. The Fermi surface at different concentrations of holes with $x=0.1$, 0.2, 0.3, 0.4, 0.5, and 0.6. Further, $t'/t=0.30$. The Fermi surfaces satisfy the Luttinger theorem.

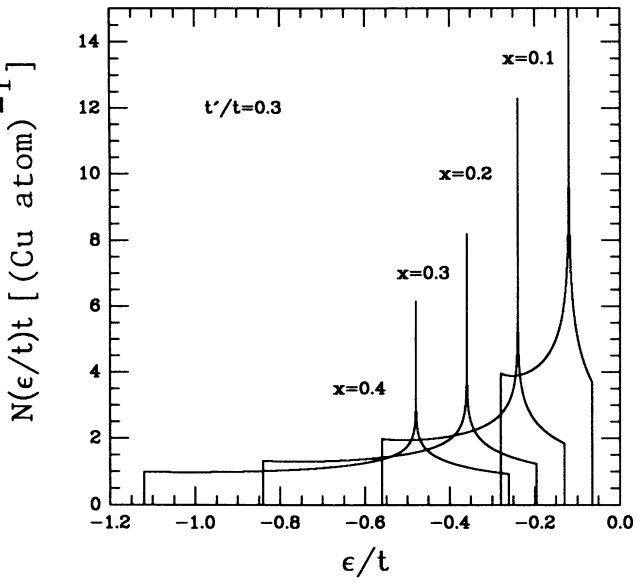

FIG. 2. The normalized density of states of quasiparticles in the lower Mott-Hubbard band (LB), $N(\varepsilon/t)t$, as a function of ε/t for $x=0.1$, 0.2, 0.3, and 0.4 and $t'/t=0.30$. One notes that the LB is broadened as the doping increases. Also note the Van Hove singularity in each curve.

with ε_u determined from Eq. (28). In Fig. 2, we have shown the normalized density of states versus normalized energy for x = 0.1, 0.2, 0.3, and 0.4 and $t'/t=0.3$. One notes that the bandwidth increases as the hole concentration increases. One also notes the existence of Van Hove singularity in each curve. Figure 3 shows the energy dependence of the density of states for $x=0.2$ and $t'/t=0.0$, 0.1, 0.2, 0.3, 0.4, and 0.5. For these values of t'/t the minimum of the LB occurs at the zone center. For $t'/t>0.5$ the band minimum occurs at zone edges $(0,\pm\pi)$, $(\pm\pi,0)$ and the Fermi surface has different topology from the cases of $t'/t<0.5$. However, different calculations indicate that for copper oxides $t'/t<0.5$ is appropriate.[10,11] One notes that the LB is narrowed as t'/t increases. Further the Van Hove singularity shifts from the upper edge to the lower edge of the LB as t'/t increases from 0.0 to 0.5. From Figs. 2 and 3 we observe that the position of the Van Hove singularity shifts uniformly as x or t'/t changes. Comparing our results with those from the two-band model, we point out that the narrowing of the band with the decrease in doping found here is similar to that found by KLA.[32] However, in the two-band calculation of NPT,[31] the band broadens as doping is reduced. In Fig. 4, the density of states at the Fermi energy is plotted as a function of hole concentration x for $t'/t=0.0$, 0.1, 0.2, 0.3, 0.4, and 0.5. One notes the Van Hove singularity for $t'/t=0.1$, 0.2, and 0.3 curves. Further, the density of states increases rapidly as x becomes less than about 0.1. This divergence in the density of states at Fermi energy as $x\to 0$ is the so-called Brinkman-Rice divergence[46] and is due to the Brinkman-Rice localization. This localization also appears in the two-band theories of KLA[32] and GKM[35] ($J=0$ case) but is absent in the theory of NPT.[31] In Ref. 35 it is found that the inclusion of the superexchange interaction treated with the RVB mean-field theory removes the Brinkman-Rice localization and also reduces the density of states by about 5 folds for moderate doping. We expect that the inclusion of the J term in our approach will mainly affect the density of states at low hole concentrations. Using the density of states at the Fermi energy given in Fig. 4, the Sommerfeld parameter γ and the zero-temperature band Pauli magnetic susceptibility χ_{SB} can be easily obtained from Eq. (25) and the relation $\chi_{SB}=\mu_B^2 N(\mu^e)$. For example, for $t=0.45$ and $t'/t=0.3$, we obtain $\gamma=23.5$, 17.7, 15.5, 15.9, and 13.7 mJ/mole K^2 and $\chi_{SB}=3.23$, 2.43, 2.13, 2.17, and 1.88 (units of 10^{-4} emu/mole), for $x=0.1$, 0.15, 0.20, 0.25, and 0.30, respec-

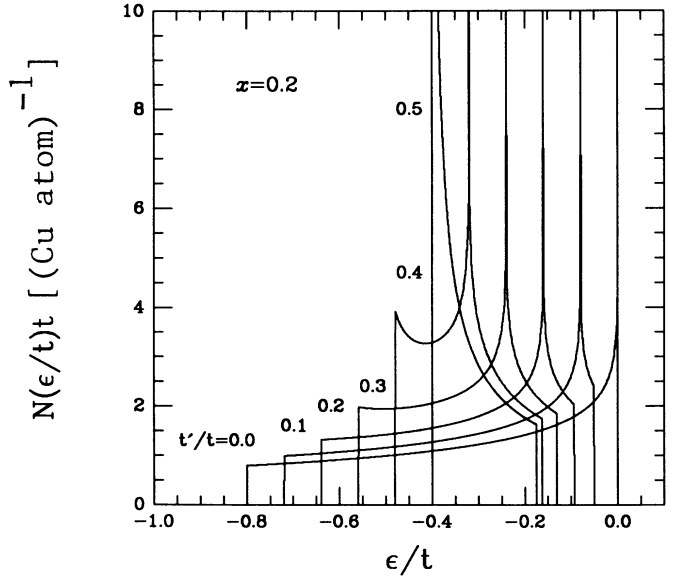

FIG. 3. The density of states $N(\varepsilon/t)t$ as a function of ε/t for $x=0.2$ and $t'/t=0.0$, 0.1, 0.2, 0.3, 0.4, and 0.5. Note that the LB is narrowed as t'/t increases. Further, the Van Hove singularity shifts from the upper edge to the lower edge of LB as t'/t increases from 0.0 to 0.5.

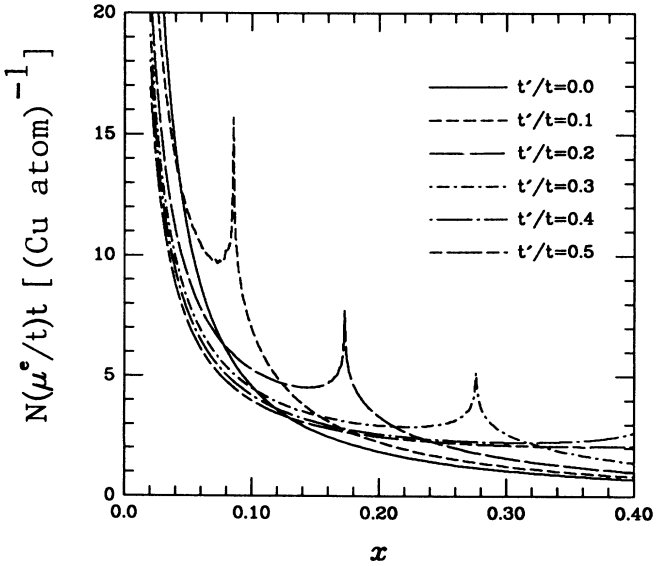

FIG. 4. The density of states at the Fermi energy as a function of x for $t'/t=0.0$, 0.1, 0.2, 0.3, 0.4, and 0.5. The divergence as $x\to 0$ is due to the Brinkman-Rice localization.[46]

tively. The measured values of γ for $YBa_2Cu_3O_7$ are in the range 7–12.5 mJ/mole K^2.[49] In the above, mole means molar plane Cu. The experimental values of χ_{SB} is in the range $(0.4-2.0)\times10^{-4}$ emu/mole. Thus there is a good agreement between the theoretical and the experimental values of γ and χ_{SB}. The Hall resistivity $R_H=\sigma_{xyz}/\sigma_{xx}^2$ can be obtained with Eqs. (18), (20), and (21). We found that R_H has a weak dependence on x. For example, R_H increases from 0.02 at $x=0.4$ to 0.96 at $x=0.02$, for $t'/t=0.3$. This theoretical result is not in accord with the low-temperature measurements. Physically, one expects that the electron distribution near the Fermi surface is smeared by the strong coupling between the electrons and holes. This interaction smearing becomes more and more important as the temperature smearing is reduced by lowering the temperature. Therefore, the present approximated treatment of the t-t'-J model works better at high temperature than at low temperature.

In Fig. 5, we have shown the Fermi energy measured relative to the lower edge of the LB for $t'/t=0.0$, 0.1, 0.2, 0.3, 0.4, and 0.5. One notes that the Fermi energy increases monotonically with the increase in the hole concentration for all the curves except the one with $t'/t=0.5$. At a fixed hole concentration, the Fermi energy decreases as t'/t increases. This decrease in the Fermi energy is caused by the narrowing of the LB and the shifting of the weight in the density of states from the upper edge to the lower edge of LB as t'/t increases from 0.0 to 0.5 (see Fig. 3).

Figure 6 shows the ratio of the effective mass at the Fermi energy to the free electron mass as calculated from Eqs. (26) and (25). We have used $t=0.45$ and $t'/t=0.0$, 0.1, 0.2, 0.3, 0.4, and 0.5. This value of t is in good agreement with the semiempirical value[10] ($t=0.4$ eV) and the value from the constrained LDA calculation ($t=0.43$ eV).[11] The effective mass shows features similar to those

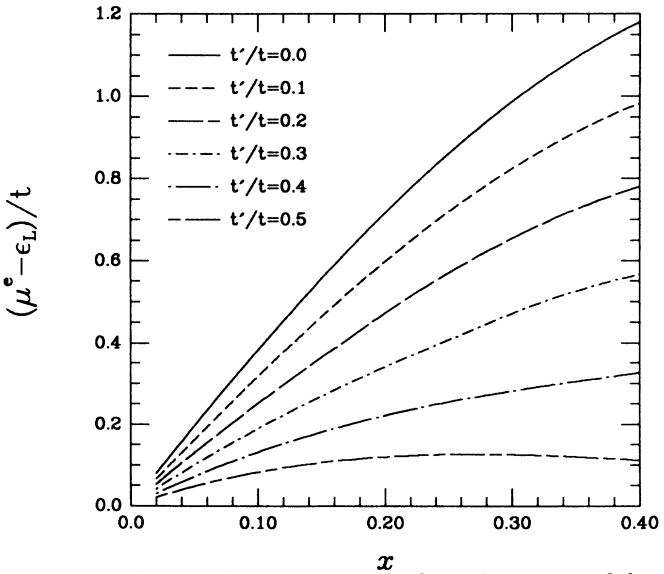

FIG. 5. The Fermi energy measured from the bottom of the LB as a function of x for $t'/t=0.0$, 0.1, 0.2, 0.3, 0.4, and 0.5. At a fixed hole concentration, the Fermi energy decreases as t'/t increases.

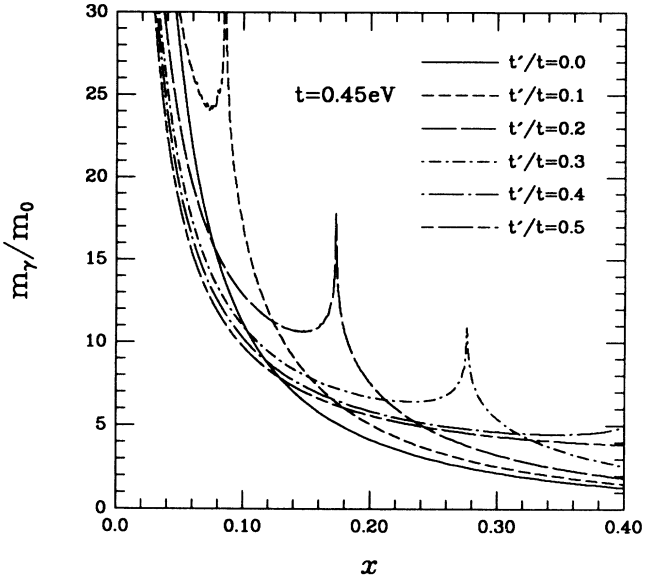

FIG. 6. The normalized effective mass m_γ/m_0 as a function of x for $t=0.45$ eV and $t'/t=0.0$, 0.1, 0.2, 0.3, 0.4, and 0.5. The effective mass is extremely anisotropic.

in the density of states at the Fermi energy. The magnitude of the effective mass is in the desired range. It may be mentioned that the effective mass is extremely anisotropic, which is due to the nonparabolic nature of the band.

The Drude plasma frequency can be calculated by using $\omega_p^2=4\pi\sigma_{xx}/\tau$ with σ_{xx} obtained from Eq. (17). ω_p^2 at zero temperature as a function of x with $t=0.45$ eV and $t'/t=0.0$, 0.1, 0.2, 0.3, 0.4, and 0.5 is shown in Fig. 7. One notes that ω_p^2 increases monotonically as the hole concentration increases. For $x<0.2$, the curves are linear in x and ω_p^2 is insensitive to the parameter t'. ω_p^2 for other values of t can be easily obtained. At present,

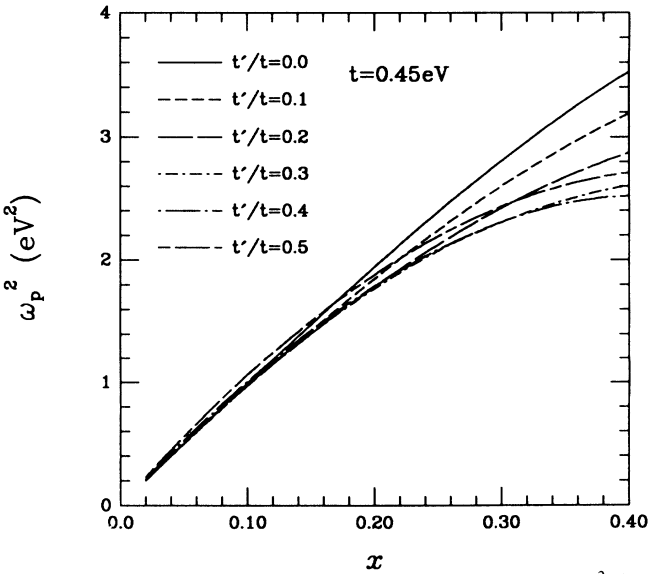

FIG. 7. The square of the Drude plasma frequency ω_p^2 (at zero temperature) as a function of x with $t=0.45$ eV and $t'/t=0.0$, 0.1, 0.2, 0.3, 0.4, 0.5. One notes the linear dependence of ω_p^2 on x for $x<0.2$.

the extraction of plasma frequency from the infrared reflectivity measurements is still controversial.[50] However, the plasma frequency for $YBa_2Cu_3O_7$ obtained from both the magnetic penetration depth and the optical measurements[51] is 1.4 eV. Using $x=0.225$ (Ref. 52) and $l_c=0.585$ Å, appropriate for $YBa_2Cu_3O_7$, we obtain $\omega_p^2=1.56$, 1.52, 1.49, 1.48, 1.48, and 1.52 $(eV)^2$ for $t'/t=0.0$, 0.1, 0.2, 0.3, 0.4, and 0.5, respectively. The agreement between the calculated and the experimental values is important as ω_p for $YBa_2Cu_3O_7$ is one of the few undisputed data. In the two-band model calculation of *GKM*,[35] ω_p^2 shows a similar doping dependence but with much smaller magnitude. In the calculation of NPT,[31] ω_p^2 changes only slightly as the hole concentration varies from zero to one. These authors found a metallic state at zero doping.

Overall, we found that at zero temperature the present calculation explains successfully the doping dependence of Drude plasma frequency. The calculation of Sommerfeld parameter γ, band Pauli magnetic susceptibility χ_{SB}, and Hall resistance R_H agrees with the experimental data for moderate doping ($x>0.1$). The calculation failed at lower doping for γ, χ_{SB}, and R_H. To remove these disagreements a refined treatment of the t-t'-J model is required.

We may mention that the present calculation predicts that the zero temperature susceptibility, mass, and γ diverge like $1/x$ as $x\rightarrow 0$, and that R_H goes to a constant. In contrast, Ref. 20 predicts that the susceptibility, mass, and γ go to a constant and that R_H diverges like $1/x$. Both calculations agree that $\omega_p^2\sim x$.

B. Transport properties at room temperature

In this part, we study the following transport properties at room temperature: Hall resistivity, band Pauli magnetic susceptibility, thermopower, and dc conductivity. Various transport properties are calculated using Eqs. (17)–(21) and (23). First we calculate ε_u from Eq. (28). With this ε_u, the Fermi energy μ^e is calculated from Eq. (27). We continue to use $t=0.45$ eV. As noted in Sec III A, this value of t is in good agreement with the values given in Refs. 10 and 11. Also it leads to a value for ω_p^2 which is in good agreement with the experimental value for $YBa_2Cu_3O_7$.

The Hall resistivity R_H is calculated from Eqs. (17), (18), and (20). Its values as a function of x at $t'/t=0.25$, 0.30, 0.35, 0.40, and 0.45 are shown in Fig. 8, along with the experimental data of Takagi *et al.*[53] ($T=270$ K) and a curve representing $R_H=x^{-1}$. The theoretical R_H has the correct sign, has very reasonable magnitude, and shows a good overall agreement with the experimental data (except for the $t'/t=0.25$ curve at low values of x).

The band Pauli magnetic susceptibility χ_{SB} is calculated from Eq. (23). The theoretical χ_{SB} as a function of hole concentration is shown in Fig. 9, where $t'/t=0.25$, 0.30, 0.35, 0.40, and 0.45 have been used. The circles represent the data of Torrance *et al.*[54] One notes that there is a qualitative agreement between the theoretical curves and the experimental data. One also notes that χ_{SB} is insensitive to t' for $x<0.1$.

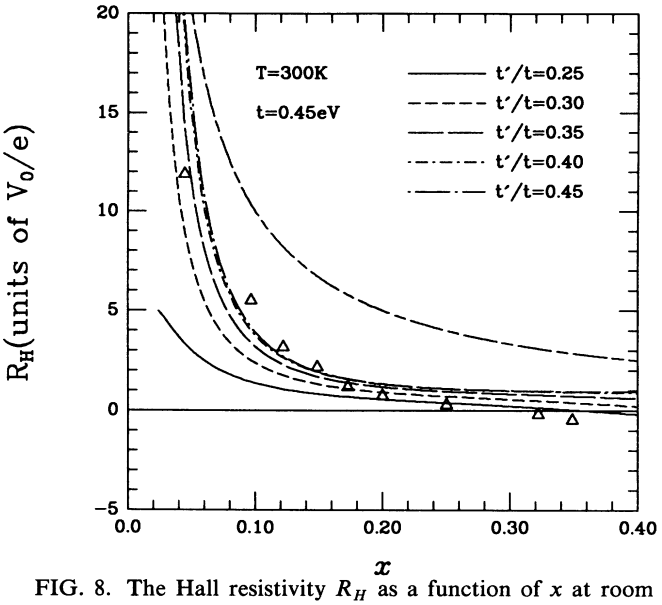

FIG. 8. The Hall resistivity R_H as a function of x at room temperature with $t=0.45$ eV and $t'/t=0.25$, 0.30, 0.35, 0.40, and 0.45. The experimental data (2:1:4 compound) of Takagi *et al.*[53] is also shown. Here $V_0=94.2$Å^3 is the volume of a formula unit. Further, $l_c=6.6$ Å. The upper short-long-dashed line represents $R_H=x^{-1}$. There is a good overall agreement between the theoretical values and the experimental data (except for $t'/t=0.25$ curve for low x).

The thermopower S is calculated from Eqs. (19) and (21) and is shown in Fig. 10 as a function of x with $t'/t=0.25$, 0.30, 0.35, 0.40, and 0.45. The experimental data[55] for Sr and Ba doping is also shown. One notes the quantitative agreement between the theoretical values and the experimental data. The theoretical S is insensitive to t' for $x<0.2$. S changes sign at $x\simeq 0.25$.

The dc-conductivity σ_{xx} is calculated from Eq. (17). The theoretical values of σ_{xx} as a function of x along

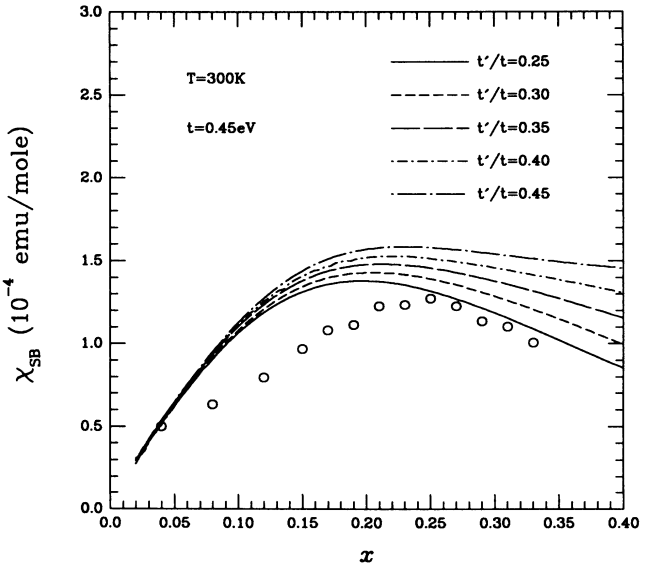

FIG. 9. The band Pauli magnetic susceptibility χ_{SB} as a function of x at room temperature with $t=0.45$ eV and $t'/t=0.25$, 0.30, 0.35, 0.40, and 0.45. The data (2:1:4 compound) of Torrance *et al.*[54] is shown as circles. Note the qualitative agreement between the theoretical curves and the experimental data.

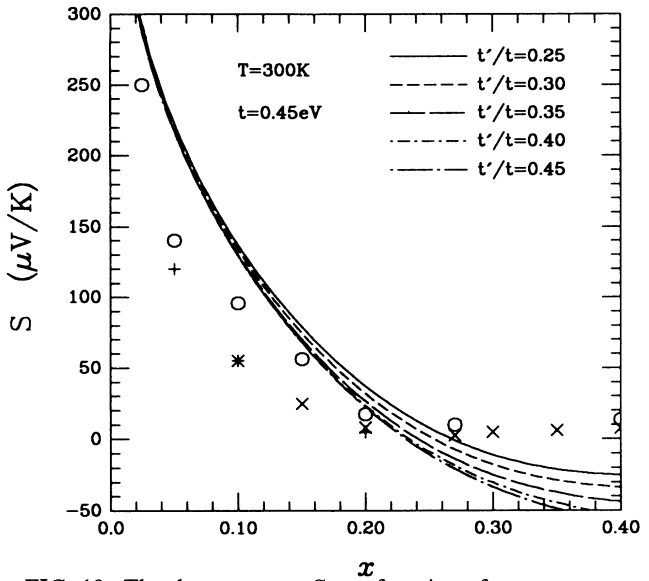

FIG. 10. The thermopower S as a function of x at room temperature with $t=0.45$ eV and $t'/t=0.25$, 0.30, 0.35, 0.40, and 0.45. The experimental data (2:1:4 compound, Ref. 55) at room temperature is shown as plusses (Cooper *et al.*) and crosses (Devaux *et al.*) for Sr doping and circles (Cooper *et al.*) for Ba doping. There is quantitative agreement between the theoretical curves and the experimental data.

with the experimental data of Torrance *et al.*[54] are shown in Fig. 11. We have used $t'/t=0.25$, 0.30, 0.35, 0.40, and 0.45. The relaxation time τ is not known and has been chosen at $1/\tau(300\text{ K}) = 2.19\times10^{14}\text{ sec}^{-1}$. One notes an excellent agreement between the theoretical and the experimental values for the entire range of x and for all values of t'/t. For $x<0.3$, σ_{xx} is nearly independent of t'/t. Here, we have assumed that τ is independent of x. The validity of this assumption will be examined in a future calculation of the relaxation time.

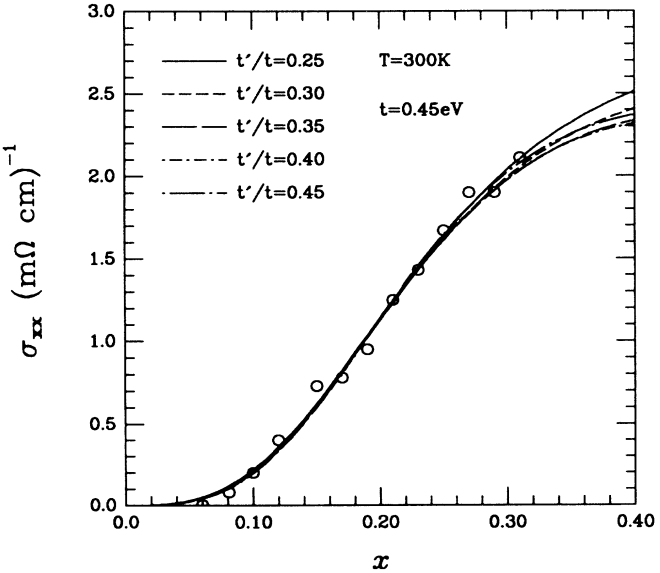

FIG. 11. The dc conductivity σ_{xx} at room temperature as a function of x, together with the experimental data (2:1:4 compound) of Torrance *et al.*[54] Here $t=0.45$ eV and $t'/t=0.25$, 0.30, 0.35, 0.40, and 0.45 have been used and the relaxation time τ has been taken as $\tau^{-1}(300\text{ K}) = 2.19\times10^{14}\text{ sec}^{-1}$. Further, $l_c=6.6$ Å. Note the excellent agreement between the theoretical and the experimental values.

Due to the relatively complex nature of the two-band-model-based calculations, only the zero-temperature Hall resistance has been calculated by KLA.[32] Their calculation provides an understanding of the doping dependence of R_H. KLA[32] remove the Brinkman-Rice[46] localization by including the interplane hopping. But, their treatment of the interplane hopping has been criticized for neglecting the strong correlation effect.[35]

C. Transport properties at various temperatures

Here we study the following properties at various temperatures: Hall resistance, band Pauli magnetic susceptibility, thermopower, and the Drude plasma frequency. We have taken $T=25$ K, 50 K, 100 K, 200 K, and 300 K. We will continue to use $t=0.45$ eV. For t'/t we choose $t'/t=0.3$ which is the average of the semiempirical value[10] ($t'/t=0.5$) and the constrained LDA calculation value ($t'/t=0.16$).[11] In Fig. 12, we have shown the calculated Hall resistance as a function of the hole concentration along with the experimental data of Tagaki *et al.*[53] One notes that the doping dependence of R_H is consistent with the experimental data for all the curves. All curves diverge as $x\to0$ and are temperature independent for $x>0.2$. However, the temperature dependence of the calculated R_H is not consistent with the experimental data. One also notes that the present calculation is successful in explaining the measured Hall resistance R_H at room temperature but fails at low temperatures. The reason for this has already been discussed in Sec. III A.

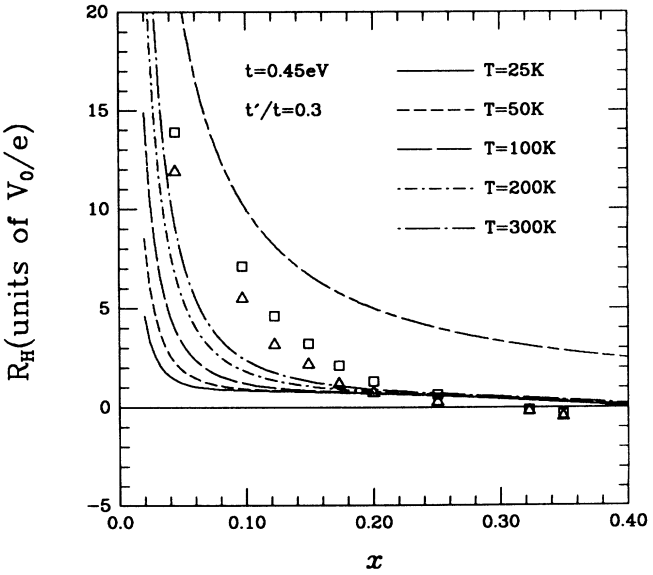

FIG. 12. The Hall resistance R_H as a function of x at $T=25$, 50, 100, 200, and 300 K. Further, $t=0.45$ eV and $t'/t=0.3$. The experimental data (2:1:4 compound) of Takagi *et al.*[53] at 80 K (squares) and 300 K (triangles) is also shown. Here $V_0=94.2$ Å^3 is the volume of a formula unit. The upper short-long-dashed line represents $R_H=x^{-1}$. Doping dependence of R_H is consistent with the experimental data, but the temperature dependence is not.

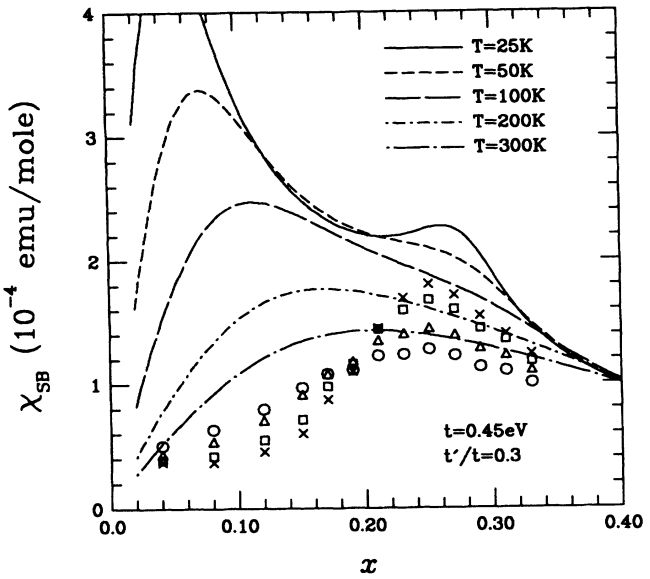

FIG. 13. The band Pauli magnetic susceptibility χ_{SB} as a function of x at $T=25$, 50, 100, 200, and 300 K. Further, $t=0.45$ eV and $t'/t=0.3$. The experimental data (2:1:4 compound) of Torrance *et al.*[54] is also shown as crosses (50 K), squares (100 K), triangles (200 K), and circles (300 K). Temperature dependence of theoretical results is consistent with the experimental data for $x>0.2$ but is not for $x<0.2$.

In Fig. 13, we have shown the band Pauli magnetic susceptibility χ_{SB} as a function of doping for various temperatures. The experimental data of Torrance *et al.*[54] is also shown. We note that while the temperature dependence of the calculated χ_{SB} is consistent with the experimental data for $x>0.2$, the temperature dependence of χ_{SB} for $x<0.2$ is wrong. However, this is not totally unexpected. χ_{SB} is a property related with the spin degree of freedom and the superexchange interaction (neglected in our study) would play an important role in its calculation.

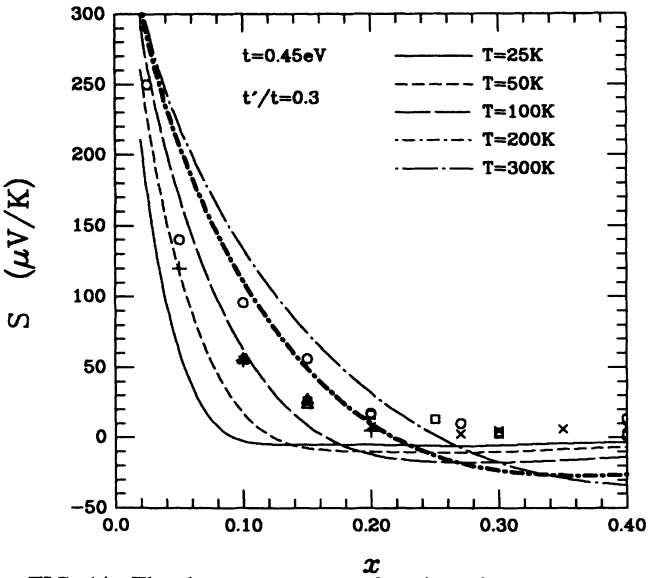

FIG. 14. The thermopower as a function of x at $T=25$, 50, 100, 200 and 300 K. Further $t=0.45$ eV and $t'/t=0.3$. The experimental data (2:1:4 compound)[55] at room temperature is shown as circles (Cooper *et al.*) for Ba doping, plusses (Cooper *et al.*) and crosses (Devaux *et al.*) for Sr doping. The experimental data[55] at 240 K is shown as squares (Ando *et al.*) for Sr doping and triangles (Ishii *et al.* for Ba doping). There is good agreement between the calculated values and experimental data.

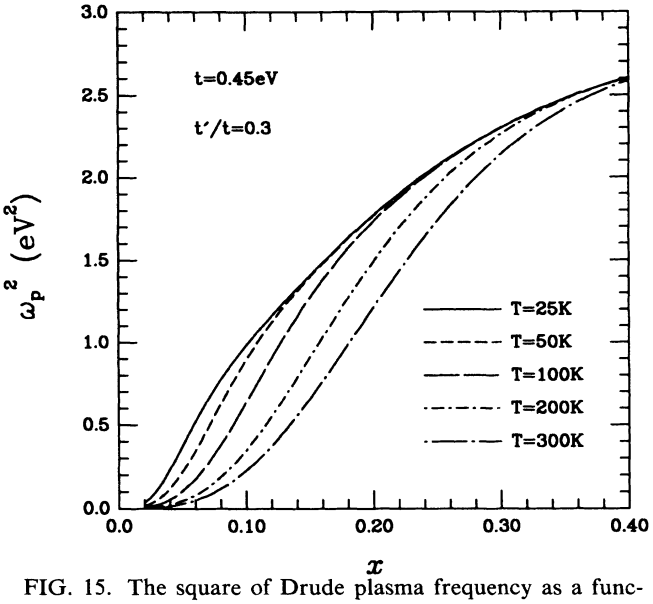

FIG. 15. The square of Drude plasma frequency as a function of x at $T=25$, 50, 100, 200 and 300 K. We have used $t=0.45$ eV and $t'/t=0.3$. Note that ω_p^2 decreased as the temperature increases.

In Fig. 14, we have plotted the calculated thermopower S as a function of x for various temperatures. Experimental data[55] of various authors are also shown. One notes a good agreement between the calculated values and the experimental data. With an increase in temperature, the theoretical S increases for $x<0.12$ and decreases for $x>0.34$.

Figure 15 shows the square of the Drude plasma frequency as a function of x for various temperatures. We note that ω_p^2 decreases as the temperature increases. The temperature dependence of ω_p^2 is more significant for $x<0.2$.

IV. SUMMARY AND DISCUSSION

In the present study, we have explained several normal state properties of the high-temperature superconductors by using a mean field theory of the t-t'-J model. We have used the slave-boson method to treat the strong correlations. Important features of the present study are that the fermion quasiparticles carry both charge and spin and that the volume of the Fermi surface satisfies the Luttinger theorem. Among other theories, those[20] based on the idea of a charged fermion hole moving in a quantum antiferromagnet do not satisfy the Luttinger theorem, and those with charge and spin deconfinement (e.g., "Luttinger liquid" theory[27] and the gauge field theory[23]) have a "spinon" Fermi surface which does satisfy the Luttinger theorem. As emphasized by Pines,[56] the data from the Knight shift[57] and the nuclear spin relaxation rate[58] give strong evidence that the quasiparticles carry both charge and spin.

Some properties at zero temperature are shown in Figs. 1–7. We find excellent agreement between the calculated

value of the Drude plasma frequency with the experimental data for $YBa_2Cu_3O_7$. The density of states, Fermi energy, the effective mass, and the Sommerfeld parameter γ have reasonable values. Detailed comparison with the experimental data can be made when the experimental data converge. Transport properties at room temperature are shown in Figs. 8–11 which provide a quantitative understanding on the doping dependence of the Hall resistivity R_H, the band Pauli magnetic susceptibility χ_{SB}, the thermopower S, and the dc conductivity σ_{xx}. The temperature dependence of the transport properties is given in Figs. 12–15. We find that the temperature dependence of R_H and χ_{SB} for $x < 0.2$ are not consistent with the experimental data. Some refinements and extensions of the present study would be needed to remove these discrepancies. Two obvious extensions are to use Eqs. (14) and (15) instead of Eq. (16) and to include the effect of the superexchange term. The contribution of the J term to χ_{SB} would be significant even in the metallic phase.

The electron-hole coupling term given in Eq. (13) can lead to superconducting pairing[45] and is also believed to be responsible for the anomalous relaxation time τ of the electrons. A calculation of τ using this coupling term is underway.

For "n-type" HTSC compounds, e.g., $Nd_{2-x}Ce_xCuO_4$, the physics occurs in the upper Mott-Hubbard band. The role of spinless neutral holes representing the vacant sites in the "p-type" HTSC systems is played by different spinless neutral bosons representing doubly occupied sites in the "n-type" systems. Further, in these compounds, the singly occupied sites are more conveniently represented by fermion holes carrying a positive charge and having an energy spectrum $\varepsilon_p^{FH} = -\varepsilon_p$. With these changes, the formalism presented in the present work can also be applied to the "n-type" systems.

Summarizing, we have studied the doping and the temperature dependence of various normal-state properties of HTSC using quasiparticle energy spectrum obtained from the mean-field treatment of the t-t'-J model. The Fermi surface satisfies the Luttinger theorem. The calculations give quantitative explanation of the doping dependence of Drude plasma frequency, Hall resistivity R_H, band Pauli magnetic susceptibility χ_{SB}, thermopower, and the room-temperature dc conductivity. The temperature dependence of R_H and χ_{SB} for small doping are not understood.

ACKNOWLEDGMENT

This work was supported in part by the Natural Sciences and Engineering Research Council of Canada.

[1] *High-Temperature Superconductivity,* edited by K. S. Bedell *et al.* (Addison-Wesley, Redwood City, CA, 1990).
[2] *Strong Correlation and Superconductivity,* edited by H. Fukuyama, S. Maekawa, and A. P. Malozemoff (Springer-Verlag, Berlin 1989).
[3] P. W. Anderson, Science **235**, 1196 (1987).
[4] P. W. Anderson, in *Frontiers and Borderlines in Many-Particle Physics,* edited by R. A. Broglia and J. R. Schrieffer (North-Holland, Amsterdam, 1988), pp. 1–40.
[5] C. M. Varma, S. Schmitt-Rink, and E. Abrahams, Solid State Commun. **62**, 681 (1987).
[6] V. J. Emery, Phys. Rev. Lett. **58**, 2794 (1987); J. E. Hirsch *ibid.* **59**, 228 (1987).
[7] V. J. Emery, Physica **B169**, 17 (1991).
[8] F. C. Zhang and T. M. Rice, Phys. Rev. B **37**, 3759 (1988).
[9] G. Kotliar, P. A. Lee, and N. Read, Physica C **153-155**, 538 (1988).
[10] L. H. Tjeng, H. Eskes, and G. A. Sawatzky, in *Strong Correlation,* Ref. 2, p. 33.
[11] M. S. Hybertsen *et al.*, Phys. Rev. B **41**, 11 068 (1990).
[12] P. A. Lee, in *Strong Correlation,* Ref. 2, pp. 23–32.
[13] W. F. Brinkman and T. M. Rice, Phys. Rev. B **2**, 1324 (1970).
[14] L. N. Bulaevskii, E. L. Nagaev, and D. I. Khomskii, Zh. Eksp. Teor. Fiz. **54** 1562 (1968) [Sov. Phys. JETP **27**, 836 (1968)].
[15] S. A. Trugman, Phys. Rev. B **37**, 1597 (1988).
[16] S. Schmitt-Rink, C. M. Varma, and A. E. Ruckenstein, Phys. Rev. Lett. **60**, 2793 (1988); F. Marsiglio, A. E. Ruckenstein, S. Schmitt-Rink, and C. M. Varma, Phys. Rev. B **43**, 10 882 (1991).
[17] C. L. Kane, P. A. Lee, and N. Read, Phys. Rev. B **39**, 6880 (1989).
[18] C. Gros and M. D. Johnson, Phys. Rev. B **40**, 9423 (1989).
[19] B. I. Shraiman and E. D. Siggia, Phys. Rev. Lett. **60**, 740 (1988).
[20] S. A. Trugman, Phys. Rev. Lett. **65**, 500 (1990).
[21] C. G. Olsen *et al.*, Phys. Rev. B **42**, 381 (1990); B. O. Wells *et al.*, Phys. Rev. Lett **65**, 3056 (1990); T. Takahaski *et al.*, Phys. Rev. B **39**, 6636 (1989); R. Manzke *et al.*, Physica C. **162-164**, 1381 (1989); J. C. Campuzano *et al.*; Phys. Rev. Lett. **64**, 2308 (1990); A. Bansil *et al.*, Phys. Rev. Lett. **61**, 2480 (1988).
[22] W. Stephan and P. Horsch, Phys. Rev. Lett. **66**, 2258 (1991).
[23] N. Nagaosa and P. A. Lee, Phys. Rev. Lett. **64**, 2450 (1990); Phys. Rev. B **43**, 1233 (1991).
[24] G. Baskaran, Z. Zou, and P. W. Anderson, Solid State Commun. **63**, 973 (1987).
[25] L. B. Ioffe and A. I. Larkin, Phys. Rev. B **39**, 8988 (1989).
[26] M. Grilli and G. Kotliar, Phys. Rev. Lett. **64**, 1170 (1990).
[27] P. W. Anderson and Y. Ren, in *High-Temperature Superconductivity,* Ref. 1, pp. 3–34.
[28] M. Ogata, T. Sugiyama, and H. Shiba, Phys. Rev. B **43**, 8401 (1991).
[29] H. Frahm and V. E. Korepin, Phys. Rev. B **43**, 5653 (1991).
[30] D. M. Newns, M. Rasolt, and P. Pattnaik, Phys. Rev. B **38**, 6513 (1988); D. M. Newns *et al.*, *ibid.* **38**, 7033 (1988); D. M. Newns and P. C. Pattnaik, in *Strong Correlation,* Ref. 2, pp. 146–166.
[31] D. M. Newns, P. C. Pattnaik, and C. C. Tsuei, Phys. Rev. B **43**, 3075 (1991).
[32] J. H. Kim, K. Levin, and A. Auerback, Phys. Rev. B **39**, 11 633 (1989).
[33] C. Castellani and G. Kotliar, Phys. Rev. B **39**, 2876 (1989).
[34] C. A. Balseiro, M. Avignon, A. G. Rojo, and B. Alascio, Phys.

Rev. Lett. **62**, 2624 (1989).
[35]M. Grilli, B. G. Kotliar, and A. J. Millis, Phys. Rev. B **42**, 329 (1990).
[36]C. M. Varma, P. B. Littlewood, S. Schmitt-Rink, E. Abrahams, and A. E. Ruckenstein, Phys. Rev. Lett. **63**, 1996 (1989).
[37]J. Ruvalds and A. Virosztek, Phys. Rev. B **43**, 5498 (1991).
[38]T. Schneider and M. P. Sörensen, Z. Phys. B **81**, 3 (1990).
[39]J. E. Hirsch, Phys. Rev. Lett. **54**, 1317 (1985).
[40]K. Chao, J. Spalek, and A. Oles, J. Phys. C **10**, L271 (1977).
[41]C. Gross, R. Joynt, and T. M. Rice, Phys. Rev. B **36**, 381 (1987).
[42]This technique was proposed by S. Barnes [J. Phys. F. **26**, 1375 (1976)], and has been developed extensively in studies of heavy fermions and high-T_c superconductivity. See P. Coleman, Phys. Rev. B **28**, 5255 (1983); **29**, 3035 (1984); **35**, 5072 (1987); N. Read and D. M. Newns, J. Phys. C **16**, 3273 (1983); D. M. Newns and N. Read, Adv. Phys. **36**, 799 (1987); A. J. Millis and P. A. Lee, Phys. Rev. B **35**, 3394 (1987); A. Auerbach and K. Levin, Phys. Rev. Lett. **57**, 877 (1986); G. Kotliar and A. E. Ruckenstein, Phys. Rev. Lett. **57**, 1362 (1986).
[43]Different schemes of assigning the charge and spin to quasiparticles such as the slave-fermion formalism [Z. Zou and P. W. Anderson, Phys. Rev. B **37**, 627 (1988)] and the Schwinger-boson–slave-fermion formalism [P. A. Lee, Phys. Rev. Lett. **63**, 680 (1989)] have also been proposed in literature.
[44]A. E. Ruckenstein, P. J. Hirschfeld, and J. Appel. Phys. Rev. B **36**, 857 (1987); M. Inui *et al.*, Phys. Rev B **37**, 2320 (1988).
[45]H. Chi and A. D. S. Nagi, Solid State Commun. **65**, 1563 (1988); Phys. Rev. B **40**, 4423 (1989); **40**, 7361 (1989).
[46]W. F. Brinkman and T. M. Rice, Phys. Rev. B **3**, 4302 (1970).
[47]J. M. Ziman, *Electrons and Phonons* (Oxford University Press, New York, 1960).
[48]P. B. Allen, W. E. Pickett, and H. Krakauer, Phys. Rev. B **37**, 7482 (1988).
[49]B. Batlogg, Physica B **169**, 7 (1991).
[50]T. Timusk and D. B. Tanner, in *Physical Properties of High-Temperature Superconductors I,* edited by D. M. Ginsberg (World Scientific, Singapore, 1989); M. Suzuki, in *Strong Correlation,* Ref. 2, pp. 280-288.
[51]B. Batlogg, in *High-Temperature Superconductivity,* Ref. 1, pp. 37-93.
[52]T. Penney, M. W. Shafer, and B. L. Olson, Physica C **162-164**, 63 (1989).
[53]H. Takagi *et al.*, Phys. Rev. B **4**, 2254 (1989).
[54]J. B. Torrance *et al.*, Phys. Rev. B **40**, 8872 (1989).
[55]J. R. Cooper *et al.*, Phys. Rev. B **35**, 8794 (1987); Y. Ando *et al.*, Solid State Commun. **70**, 303 (1989); H. Ishii *et al.*, Physica **148B**, 419 (1987); F. Devaux *et al.*, Phys. Rev. B **41**, 8723 (1990).
[56]D. Pines, in *High-Temperature Superconductivity,* Ref. 1, pp. 240–245.
[57]S. E. Barrett, *et al.*, Phys. Rev. B **41**, 6283 (1990); M. Takigawa *et al.*, Phys. Rev. B **39**, 7371 (1989).
[58]W. W. Warren *et al.*, Phys. Rev. Lett. **62**, 1193 (1989); P. C. Hammel *et al.*, Phys. Rev. Lett. **63**, 1992 (1989); T. Imai *et al.*, Physica C **162-164**, 169 (1989).